

Supplemental Information**Lamin B receptor recognizes specific modifications of histone H4 in heterochromatin formation**

Yasuhiro Hirano, Kohji Hizume, Hiroshi Kimura, Kunio Takeyasu,
Tokuko Haraguchi and Yasushi Hiraoka

SUPPLEMENTAL EXPERIMENTAL PROCEDURE

Calculation of the molar ratio of LBR to histone - To determine the amount of LBR within a nucleus, quantitative Western blotting was carried out according to Holaska *et al.* (1) with some modifications. HeLa cells were lysed with Laemmli's SDS sample buffer, and aliquots of the cell lysate, equivalent to 2.5×10^4 and 5.0×10^4 cells, were subjected to SDS-PAGE along with 2, 5, 10 and 20 ng [70.1, 175, 350 and 701 fmol (10^{-15} mol), respectively] of recombinant purified His-tagged NP^{WT}. After transfer to PVDF membrane, LBR protein was probed with anti-LBR antibody and quantified by comparing the staining with that of the control recombinant protein. According to Fig. S6, we determined there was 399 fmol of LBR in 5.0×10^4 HeLa cells. Based on this evaluation, we further estimated the concentration of LBR beneath the nuclear envelope as follows. We estimated the size of the nucleus as a sphere 20 μm in diameter, and defined its interaction zone (IZ) (1) within a region of 20 nm from the inner nuclear membrane (INM) as a globular protein of 24 kDa (equal to the molecular weight of the nucleoplasmic region of LBR), which was estimated to be nearly 20 nm in size. The volume of LBR's IZ (V_{IZ}) was estimated to be 25.1 fl (10^{-15} liters).

The amount of core histone was estimated as follows. It has been reported that chromatin of eukaryotes contains nearly equal weights of histone and DNA (2). In the case of human cells, one cell possesses approximately 6.0 pg of DNA. This amount is equal to 56 amol (10^{-18} mol) of histone octamer (molecular weight: 108 kDa). If histone is distributed uniformly in the 20 μm -diameter nucleus, the concentration would be approximately 13 μM . The ratio of the fluorescence intensity of DNA stained with DAPI around the NE to that of an intra-region of the nucleus was 5.8:1 (data not shown). Then, the concentration of core histone in the IZ was estimated at about 75 μM .

The concentration of LBR and that of core histone in the IZ were estimated to be 318 and 75.4 μM , respectively, as shown above (also see Holaska *et al.* (1)). Therefore, the molar ratio of LBR to histone in the IZ region is estimated to be 4:1.

SUPPLEMENTAL FIGURE LEGENDS

Fig. S1. Cellspot histone peptide array data. (A) Cellspot was incubated with NP^{WT} for 1.5 h, washed, and then probed with anti-GST antibody. Blue, red and yellow regions indicate spots containing histone H3, H4 and H2A/B-related peptides, respectively. (B) Modified histone peptides on

each spot, located on the listed spot numbers, in (A) are shown. Details of the complete matrix of peptides are provided as supplemental table S1 on the *J. Biol. Chem.* website. Black staining of the spots indicates binding to NP^{WT}. In Figure 1d, green regions are indicated.

Fig. S2. Loss of histone modification-specific binding activity in NK^{W16A}. Celluspot was incubated with NP^{W16A} for 1.5 h, washed, and then probed with anti-GST antibody. Blue, red and yellow regions indicate spots containing histone H3, H4 and H2A/B-related peptides, respectively. An overexposed image is shown in the lower panel.

Fig. S3. Molar ratio of LBR to histones. (A) Quantification of LBR in HeLa cells. The cell lysates, equivalent to 2.5×10^4 and 5.0×10^4 cells, and a recombinant His-tagged NP^{WT} protein (70.1, 175, 350, 701×10^{-15} mol) were separated by SDS-PAGE, transferred to PVDF, and probed with anti-LBR antibody. The amount of LBR in 5.0×10^4 HeLa cells was estimated as 399 fmol. (B) The diagram shows how the volume of a 20 nm IZ region near the INM of a 20 μ m-diameter nucleus was calculated; the concentration of LBR and of core histones in the IZ were estimated as 318 and 75.4 μ M, respectively (see Methods and also Holaska *et al.* (1)). Therefore, the molar ratio of LBR to histone in the IZ region is estimated to be 4:1.

Fig. S4. AFM images of the aggregated chromatin induced by NP^{WT}. Chromatin was reconstituted using 1.8 kbp linear dsDNA. After incubation with GST (A), NP^{WT} (B), NP^{W16A} (C) and Tud^{WT} (D), the chromatin structure was observed by AFM. Two μ m square regions are shown. Arrows indicate highly aggregated chromatin formed by NP^{WT}. Bars, 500 nm.

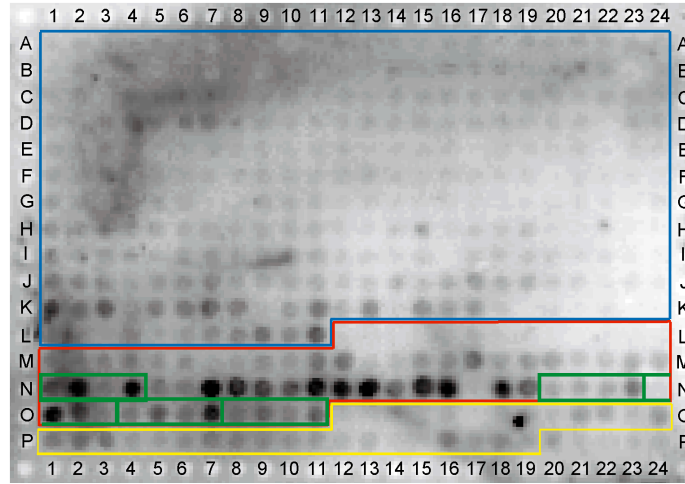
Fig. S5. NP^{WT} induced aggregation with 26 kbp chromatin as well as with 1.8 kbp chromatin. Chromatin was reconstituted using 26 kbp plasmid dsDNA. After incubation with GST (A), NP^{WT} (B), NP^{W16A} (C) and Tud^{WT} (D), the chromatin structure was observed by AFM. Bars, 500 nm.

SUPPLEMENTAL REFERENCES

1. Holaska, J. M., Lee, K. K., Kowalski, A. K., and Wilson, K. L. (2003) *J. Biol. Chem.* **278**(9), 6969-6975
2. Kornberg, R. D. (1974) *Science* **184**(139), 868-871

Figure S1

A



 : H3-related peptides : H4-related peptides
 : H2A/B-related peptides

B

	spot number	sequence	portion	modification				N-terminus
				1st	2nd	3rd	4th	
K20-related peptides	N1	GKGGAKRHRKme1VLRDNIQGIT	H4 11-30	K20me1				acetylated
	N2	GKGGAKRHRKme2VLRDNIQGIT	H4 11-30	K20me2				acetylated
	N3	GKGGAKRHRKme3VLRDNIQGIT	H4 11-30	K20me3				acetylated
	N4	GKGGAKRHRKacVLRDNIQGIT	H4 11-30	K20ac				acetylated
	N20	GKGGAKRHRme2aKme1VLRDNIQGIT	H4 11-30	R19me2a	K20me1			acetylated
	N21	GKGGAKRHRme2aKme2VLRDNIQGIT	H4 11-30	R19me2a	K20me2			acetylated
	N22	GKGGAKRHRme2aKme3VLRDNIQGIT	H4 11-30	R19me2a	K20me3			acetylated
	N23	GKGGAKRHRme2aKacVLRDNIQGIT	H4 11-30	R19me2a	K20ac			acetylated
	N24	GKGGAKRHRme2sKme1VLRDNIQGIT	H4 11-30	R19me2s	K20me1			acetylated
	O1	GKGGAKRHRme2sKme2VLRDNIQGIT	H4 11-30	R19me2s	K20me2			acetylated
	O2	GKGGAKRHRme2sKme3VLRDNIQGIT	H4 11-30	R19me2s	K20me3			acetylated
K12&K16-related peptides	L12	SGRGKGGKGLGKGGAKRHR	H4 1-19	Unmod				free
	L18	SGRGKGGKGLGKGGAKRHR	H4 1-19	K12ac				free
	L19	SGRGKGGKGLGKGGAKRHR	H4 1-19	K16ac				free
	M4	SGRGKGGKacGLGKacGGAKRHR	H4 1-19	K8ac	K12ac			free
	M5	SGRGKGGKacGLGKGGAKacRHR	H4 1-19	K8ac	K16ac			free
	M6	SGRGKGGKacGLGKacGGAacRHR	H4 1-19	K12ac	K16ac			free
	M11	SGRGKacGGKacGLGKacGGAKRHR	H4 1-19	K5ac	K8ac	K12ac		free
	M12	SGRGKGGKacGLGKacGGAacRHR	H4 1-19	K8ac	K12ac	K16ac		free
	M15	SRme2sGKacGGKacGLGKacGGAKRHR	H4 1-19	R3me2s	K5ac	K8ac	K12ac	free
	M16	SRme2sGKacGGKacGLGKacGGAKRHR	H4 1-19	R3me2s	K5ac	K8ac	K12ac	free
	M17	SGRGKacGGKacGLGKacGGAacRHR	H4 1-19	K5ac	K8ac	K12ac	K16ac	free
M18	GKGGAKRHRKVLVDNIQGIT	H4 11-30	Unmod				acetylated	
M19	GKacGGAKRHRKVLVDNIQGIT	H4 11-30	K12ac				acetylated	
M20	GKGGAKacRHRKVLVDNIQGIT	H4 11-30	K16ac				acetylated	
N7	GKacGGAacRHRKVLVDNIQGIT	H4 11-30	K12ac	K16ac			acetylated	
N8	GKGGAKacRme2sHRKVLVDNIQGIT	H4 11-30	K16ac	R17me2s			acetylated	
N9	GKGGAKacRme2aHRKVLVDNIQGIT	H4 11-30	K16ac	R17me2a			acetylated	
N10	GKGGAKacRHRme2sKVLVDNIQGIT	H4 11-30	K16ac	R19me2s			acetylated	
N11	GKGGAKacRHRme2aKVLVDNIQGIT	H4 11-30	K16ac	R19me2a			acetylated	
N12	GKGGAKacRHRKme1VLRDNIQGIT	H4 11-30	K16ac	K20me1			acetylated	
N13	GKGGAKacRHRKme2VLRDNIQGIT	H4 11-30	K16ac	K20me2			acetylated	
N14	GKGGAKacRHRKme3VLRDNIQGIT	H4 11-30	K16ac	K20me3			acetylated	
N15	GKGGAKacRHRKacVLRDNIQGIT	H4 11-30	K16ac	K20ac			acetylated	
N16	GKacGGAacRHRKme1VLRDNIQGIT	H4 11-30	K12ac	K16ac	K20me1		acetylated	
N17	GKacGGAacRHRKme2VLRDNIQGIT	H4 11-30	K12ac	K16ac	K20me2		acetylated	
N18	GKacGGAacRHRKme3VLRDNIQGIT	H4 11-30	K12ac	K16ac	K20me3		acetylated	
N19	GKacGGAacRHRKacVLRDNIQGIT	H4 11-30	K12ac	K16ac	K20ac		acetylated	

Figure S2

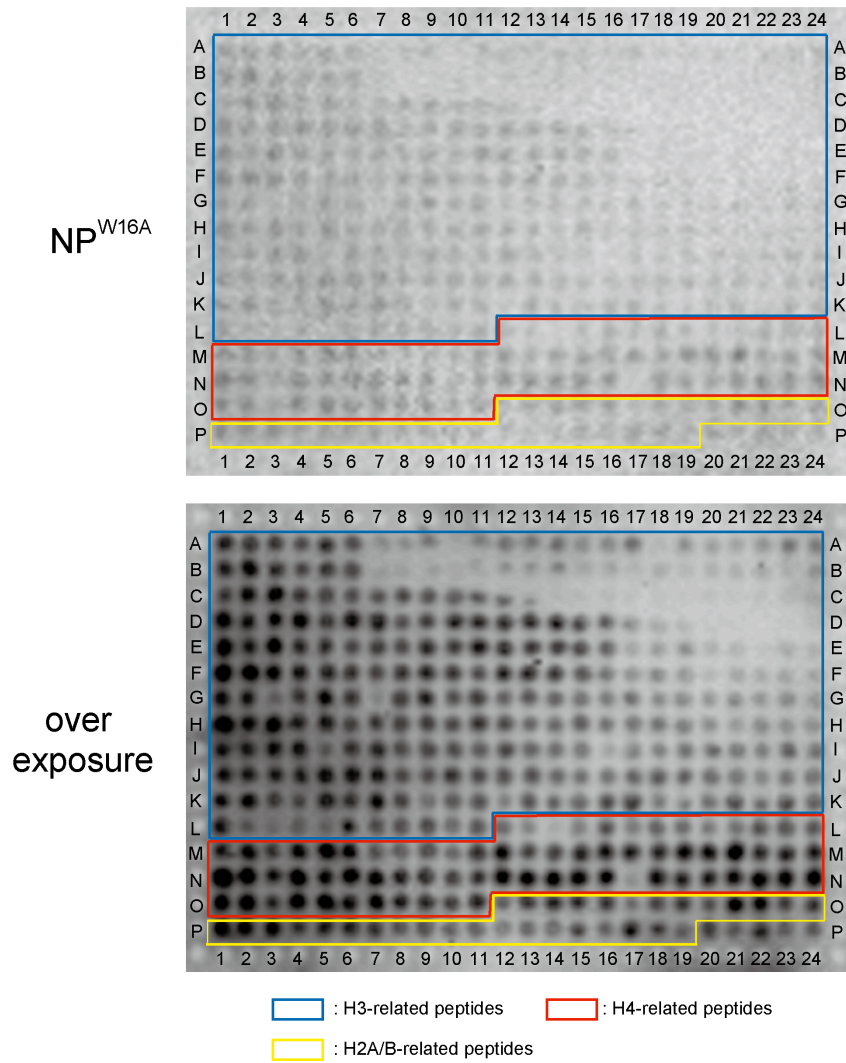


Figure S3

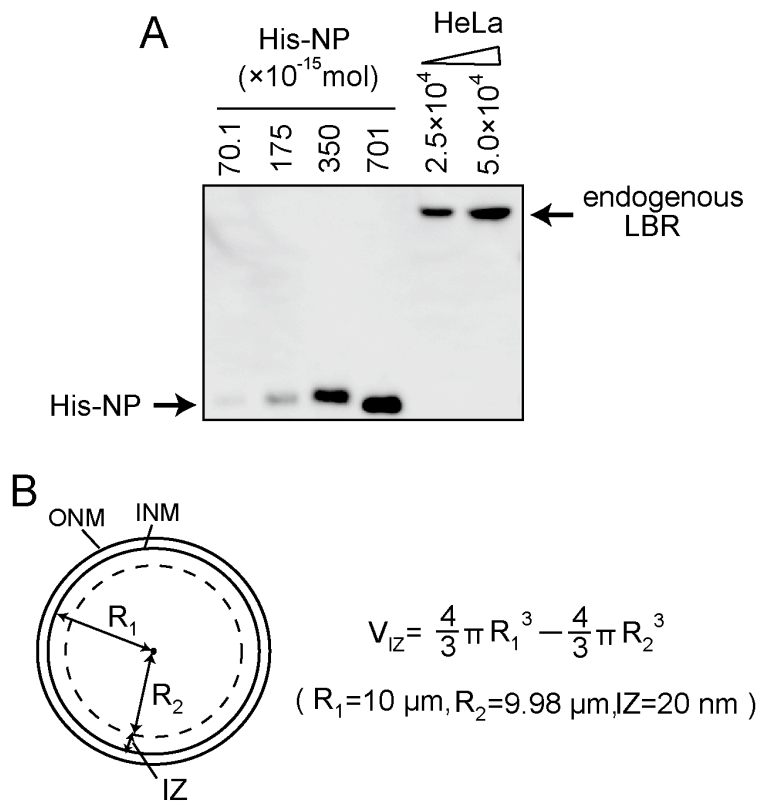


Figure S4

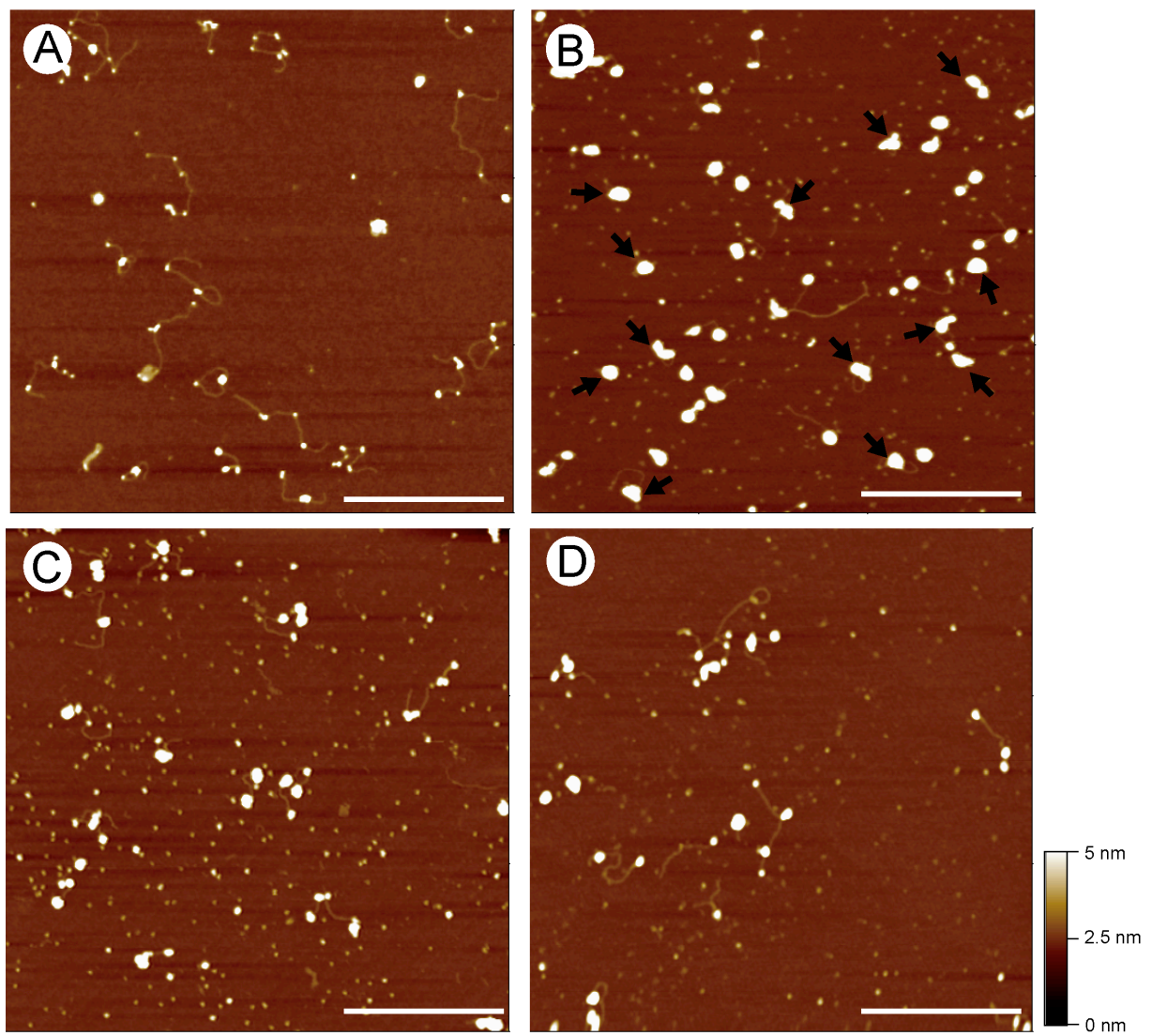


Figure S5

